

4 | Fiji



4.1 Summary

4.1.1 Climate

- Changes in air temperature from season to season are relatively small and strongly linked to changes in the surrounding ocean temperature. Fiji has two distinct seasons – a warm wet season from November to April and a cooler dry season from May to October.
- The seasonal cycle is strongly affected by the South Pacific Convergence Zone (SPCZ), which is most intense during the wet season.
- Annual and seasonal air temperatures at Suva and Nadi Airport increased over the period 1951–2020. The number of hot days and warm nights has increased at Suva and Nadi Airport, while the number of cool days and cold nights has decreased.
- The energy required for cooling indoor environments has increased at Suva and Nadi Airport, and the difference between daytime and night-time temperatures has decreased at Nadi Airport.
- There has been little change in annual, seasonal and extreme rainfall at Suva and Nadi Airport.
- Tropical cyclones usually affect Fiji between November and April. Over the period 1969–2018, an average of 28 cyclones passed within the Fiji exclusive economic zone (EEZ) per decade. Tropical cyclones were most frequent in El Niño years and least frequent in La Niña years. Year-to-year variability is large, ranging from no tropical cyclones in some seasons to six.
- There has been little change in the total number of tropical cyclones in the Southwest Pacific since 1981/82. The number of severe tropical cyclones has declined over the same period/region.

4.1.2 Ocean

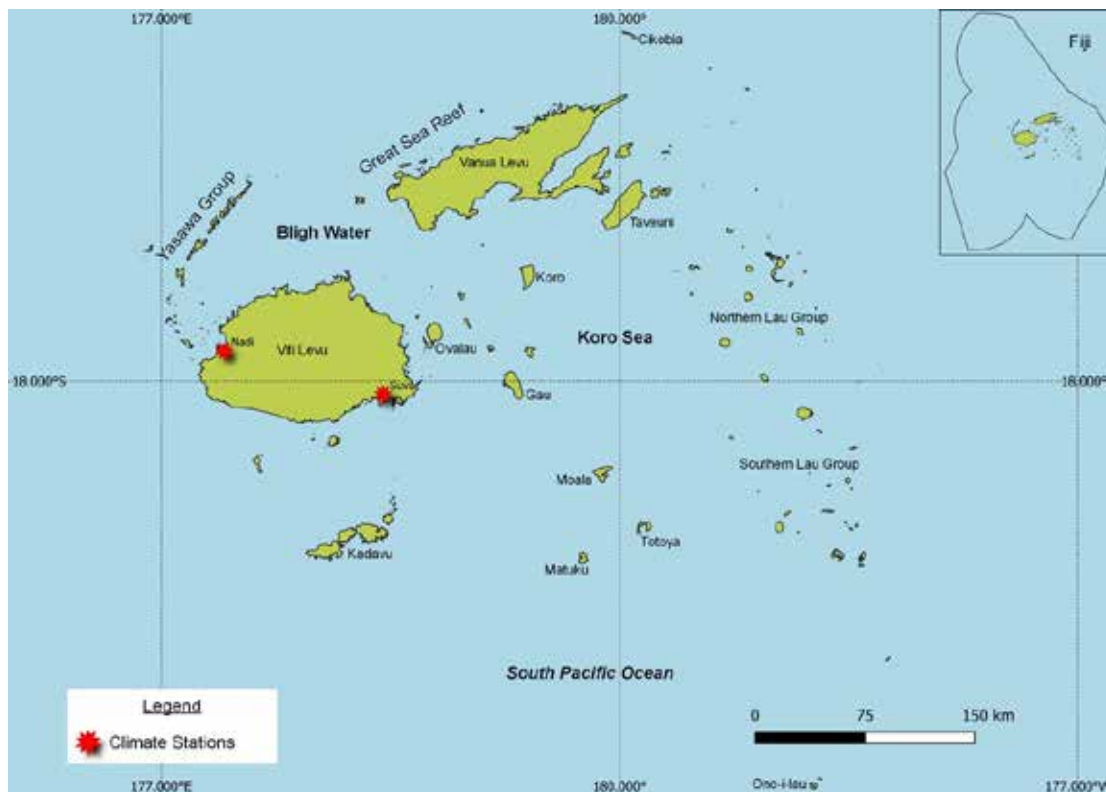
- Highest sea levels typically occur in the months October to March. La Niña brings noticeably higher sea levels outside the austral summer, specifically March/April and September/October.
- Sea-level rise within the EEZ, measured by satellite altimeters from 1993 to mid-2020, ranges from 4 to 5 mm per year, with highest trend estimates in the far north.
- Monthly average ocean temperature, as measured by the Lautoka tide-gauge, ranges from 26.4 °C in August to 30 °C in December to March. However, monthly temperatures in any given year can be up to ± 2 °C of these averages.
- The sea surface temperature (SST) trend in the EEZ is 0.26 °C per decade.
- Highest waves at Fiji occur in the winter (June–August) months, with a distinct lull during summer (December–February).
- Dominant wave direction is from 185° (south), with an average significant wave height of 0.88 m and average wave period of 12.67 s.
- Severe wave height is defined as 1.97 m, with an average of 2.7 severe events per year.
- Peak average significant wave height occurs during the austral winter.

4.2 Country description

The Republic of Fiji is located in the tropical South Pacific Ocean between latitudes 12°S and 21°S, and longitudes 176°E and 178°W (Figure 4.1). Fiji is an archipelago of more than 330 islands, of which about 110 are permanently inhabited. There are more than 500 islets. Fiji has a total land area of 18,272 km² and an EEZ of 1.3 million km².

The two largest islands are Viti Levu and Vanua Levu, which account for 87.5% of the land area. The other islands consist of small volcanic islands, low-lying atolls and elevated reefs. The highest elevation is 1324 m above sea level on Viti Levu. Fiji's population is approximately 885,000. About 87% of the population live on the two main islands.

Figure 4.1:
Fiji and the locations of the climate stations used in this report



4.3 Data

Daily historical rainfall and air temperature records for Laucala Bay, Suva and Nadi Airport from 1951 were obtained from the Fiji Meteorological Service. These records have undergone data quality and homogeneity assessment. Where the maximum or minimum air temperature records were found to have discontinuities, these records have been adjusted to make them homogeneous (further information is provided in Chapter 1). Additional information on historical climate trends for Fiji can be found in the Pacific Climate Change Data Portal <http://www.bom.gov.au/climate/pccsp>.

Tropical cyclone data and historical tracks starting from the 1969/70 season are available from the SHTC Data Portal <http://www.bom.gov.au/cyclone/history/tracks/index.shtml>.

SST covering the EEZ was obtained via the daily Optimum Interpolation SST version 2.1 (OISST v2.1) dataset from NOAA

(Reynolds et al. 2007; Banzon et al. 2016). In situ ocean temperature data were obtained from the PSLGM Project tide-gauge located at Lautoka, with data spanning from 1992 to 2021. The primary PSLGM tide-gauge in Fiji is located at Lautoka and has a longer data record than the tide-gauge at Suva.

Wave data were obtained from the PACCSAP wave hindcast (Smith et al. 2021), available hourly from 1979 to 2021, and for a grid resolution near Fiji of 7 km.

Regional sea level data were obtained from CSIRO satellite altimetry (updated by Benoit Legresy, Church and White 2011), with correction for seasonal signals, inverse barometer effect and glacial isostatic adjustment. Tide-gauge data were sourced from the Lautoka tide-gauge station, spanning from 1992 to 2021 at hourly intervals.

4.4 Rainfall

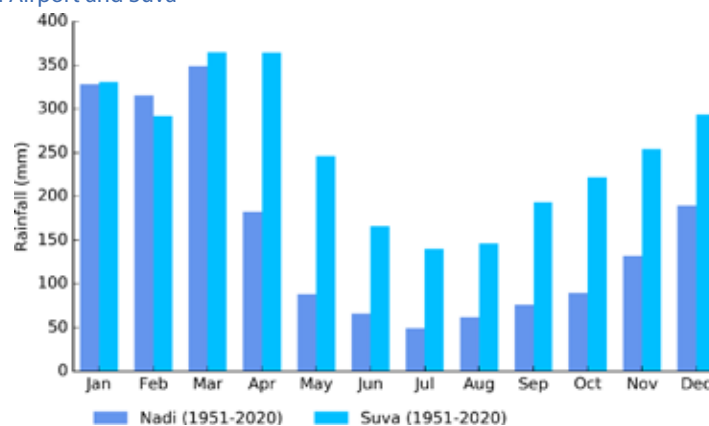
4.4.1 Seasonal cycle

In the cooler/drier half of the year (May–October), less energy is received from the sun and subtropical high-pressure systems move north bringing cooler, drier conditions. During the wetter/warmer half of the year, the SPCZ is most active and the southern edge usually lies close to Fiji, leading to about 63% of Suva’s and 78% of Nadi Airport’s rain falling during this period (Figure 4.2).

The effects of large-scale climate features such as the SPCZ and trade winds are modified on some islands due to the influence

of mountains. Those regions exposed to the trade winds can receive mean annual rainfall in excess of 4000 mm, while leeward regions to the northwest receive on average less than 2000 mm annually, with less than 25% of annual rainfall between May and October. Several weather features have a notable impact on Fiji’s climate. Active phases of the Madden–Julian Oscillation (MJO) near Fiji can be associated with significant rainfall for several days in the wet season. In addition, late afternoon convective thunderstorms contribute significant rainfall to the central and western parts of Viti Levu. In the dry season, cold fronts, which are usually weak by the time they reach Fiji’s latitude, occasionally merge with troughs in the upper atmosphere, resulting in widespread rainfall.

Figure 4.2:
Mean annual rainfall at Nadi Airport and Suva



4.4.2 Trends

Trends in annual and seasonal rainfall since 1951 are not statistically significant at Suva and Nadi Airport (Figure 4.3, Table 4.1). Annual and seasonal rainfall trends indicate little change at these sites. Notable year-to-year variability

associated with El Niño–Southern Oscillation (ENSO) is evident at Nadi Airport, with higher rainfall typically occurring during La Niña years compared to El Niño years (Figure 4.3). Annual rainfall since 1951 has varied from approximately 1600 to 4400 mm at Suva and from approximately 900 to 3500 mm at Nadi Airport.

Figure 4.3:

Annual rainfall (bar graph) and number of wet days (where rainfall is at least 1 mm; line graph) at Suva (left) and Nadi Airport (right). Straight lines indicate linear trends for annual rainfall (in black) and number of wet days (in blue). The magnitudes of the trends are presented in Table 4.1.

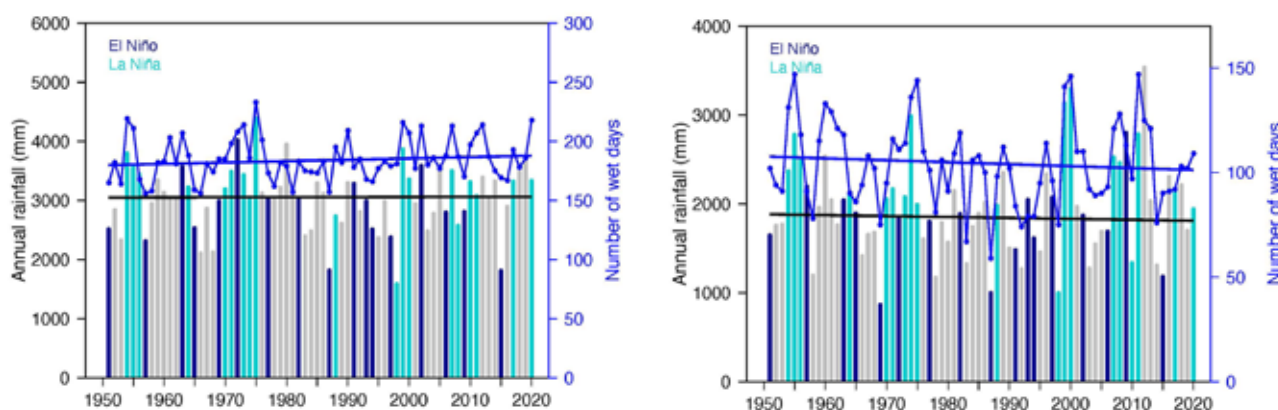


Table 4.1:

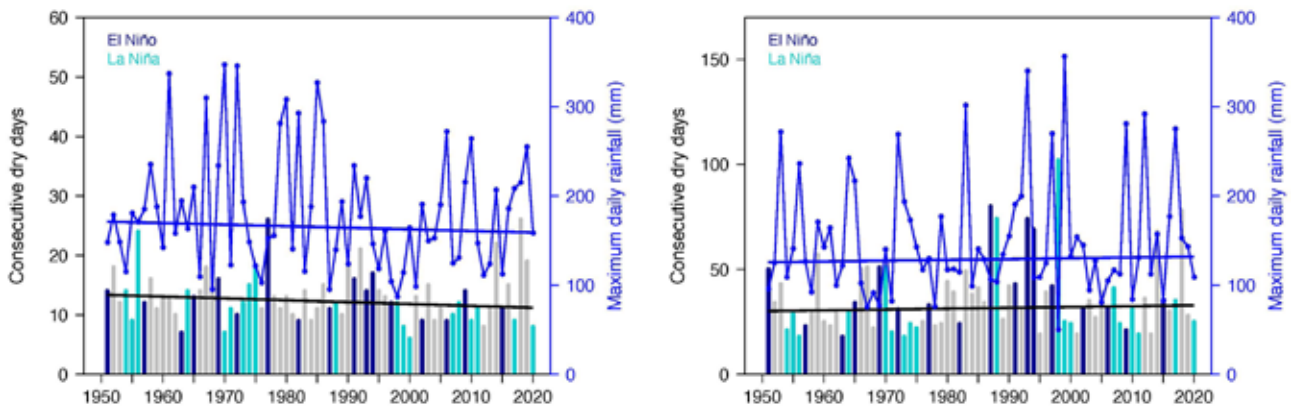
Trends in annual, seasonal and extreme rainfall at Suva (left) and Nadi Airport (right). The 95% confidence intervals are shown in parentheses. The contribution to total rainfall from extreme events and the standardised rainfall evapotranspiration index are measured relative to 1961–1990 (see Chapter 1 for details).

	Suva	Nadi Airport
	1951–2020	
Annual rainfall (mm/decade)	+1.76 (-68.20, +68.79)	-10.53 (-92.75, +75.19)
November–April (mm/decade)	-13.33 (-74.06, +46.91)	+11.92 (-51.27, +74.66)
May–October (mm/decade)	+1.30 (-51.81, +48.18)	-4.59 (-25.90, +21.75)
Number of wet days (days/decade)	+1.13 (-1.71, +3.72)	-0.93 (-4.45, +2.80)
Contribution to total rainfall from extreme events (%/decade)	-0.53 (-1.63, +0.66)	+0.71 (-0.67, +2.21)
Consecutive dry days (days/decade)	-0.31 (-0.73, 0)	+0.40 (-1.10, +2.28)
Maximum one-day rainfall (mm/decade)	-1.76 (-9.33, +5.04)	+0.89 (-4.97, +6.44)
Standardised rainfall evapotranspiration index (November–April)	-0.03 (-0.16, +0.10)	+0.02 (-0.14, +0.18)
Standardised rainfall evapotranspiration index (May–October)	+0.02 (-0.13, +0.15)	-0.01 (-0.15, +0.13)

Like annual and seasonal rainfall, no significant trends in extreme rainfall indices, including the standardised rainfall evapotranspiration drought index, were detected (Table 4.1). Figure 4.4 shows change and variability in the longest run of

days without rain and maximum daily rainfall at Suva and Nadi Airport. Nadi Airport experiences longer dry spells compared to Suva, and both sites experience high interannual variability in maximum daily rainfall.

Figure 4.4: Annual longest run of consecutive dry days (bar graph) and maximum daily rainfall (line graph) at Suva (left) and Nadi Airport (right). Straight lines indicate linear trends for dry days (in black) and maximum daily rainfall (in blue). The magnitudes of the trends are presented in Table 4.1.



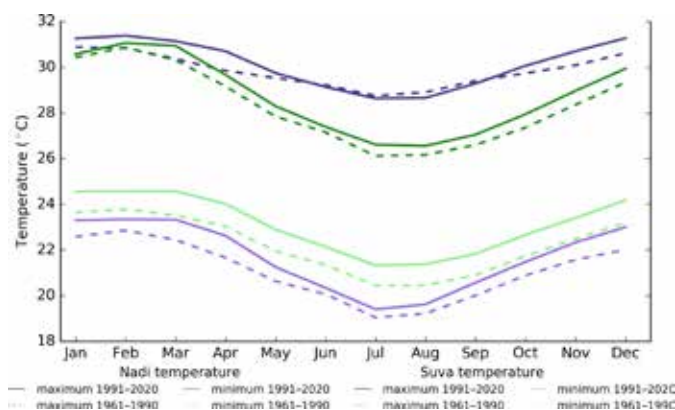
4.5 Air temperature

4.5.1 Seasonal cycle

The range in average monthly maximum temperatures throughout the year is about 5 °C for Suva and 3 °C for Nadi Airport. The average monthly minimum temperature range is about 3 °C for Suva and 4 °C for Nadi Airport for 1991–2020. There has been a clear shift towards warmer average monthly temperatures between the

climatology periods of 1961–1990 and 1991–2020 (Figure 4.5), with warmer average temperatures occurring in all months throughout the year for both Suva and Nadi Airport, with the exception of average maximum temperatures at Nadi Airport between June and September. The largest increase in average monthly temperatures for both locations occurs at the end of the warmer/wetter season (November to April).

Figure 4.5: Maximum and minimum air temperature seasonal cycle for Nadi Airport (purple) and Suva (green), and for the periods 1961–1990 (dotted lines) and 1991–2020 (full lines)



4.5.2 Trends

Average annual and seasonal temperatures have increased significantly at Suva and Nadi Airport (Figure 4.6). November–April temperatures are increasing faster than May–October temperatures at Nadi Airport (Table 4.2).

Figure 4.6: Average annual, November–April and May–October temperatures for Suva (left) and Nadi Airport (right). Straight lines indicate linear trends. The magnitudes of the trends are presented in Table 4.2. Diamonds indicate years with insufficient data for one or more variables.

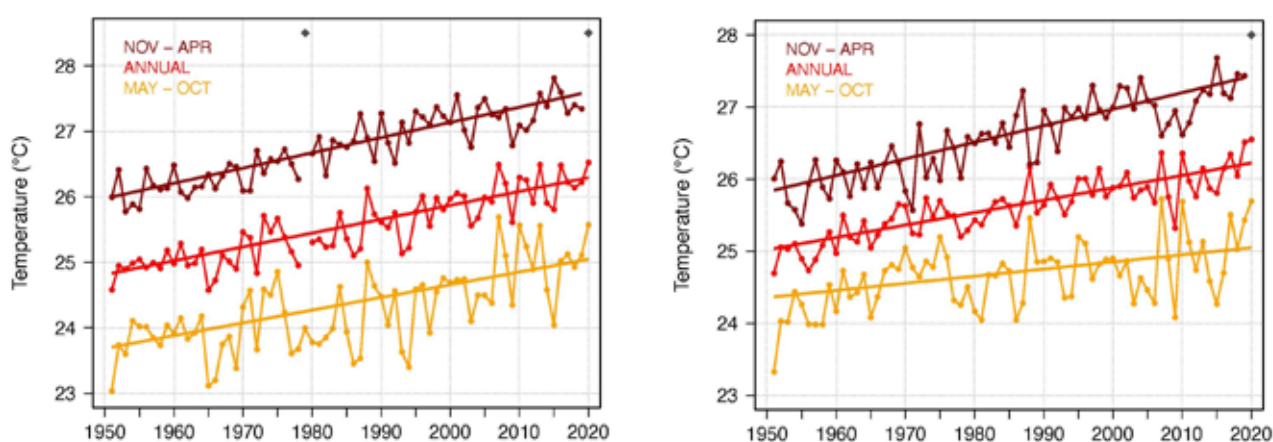


Table 4.2: Trends in annual and seasonal air temperatures at Suva (top) and Nadi Airport (bottom). The 95% confidence intervals are shown in parentheses, and trends significant at the 95% level are shown in bold.

	Suva Tmax (°C/decade)	Suva Tmin (°C/decade)	Suva Tmean (°C/decade)	Nadi Airport Tmax (°C/10yrs)	Nadi Airport Tmin (°C/10yrs)	Nadi Airport Tmean (°C/10yrs)
1951–2020						
Annual	+0.18 (+0.13, +0.23)	+0.24 (+0.19, +0.30)	+0.21 (+0.18, +0.25)	+0.15 (+0.11, +0.19)	+0.20 (+0.16, +0.24)	+0.17 (+0.15, +0.2)
November–April	+0.21 (+0.15, +0.27)	+0.26 (+0.22, +0.30)	+0.23 (+0.20, +0.26)	+0.22 (+0.16, +0.28)	+0.25 (+0.22, +0.28)	+0.23 (+0.19, +0.27)
May–October	+0.15 (+0.08, +0.22)	+0.24 (+0.15, +0.33)	+0.19 (+0.12, +0.26)	+0.07 (+0.01, +0.14)	+0.16 (+0.07, +0.23)	+0.10 (+0.05, +0.16)

The number of hot days and warm nights has increased, and the number of cool days and cold nights has decreased at Suva and Nadi Airport (Table 4.3). Increases in heat extremes have been particularly strong at Nadi Airport, with multiple recent years experiencing over 100 hot days (Figure 4.7).

The cooling degree days index provides a measure of the energy demand needed to cool a building down to 25 °C, with the assumption that air conditioners are generally turned on at this

temperature. At Suva and Nadi Airport, there has been a strong increase in the cooling degree day index, suggesting the energy needed for cooling has increased significantly since 1951. The difference between daytime and night-time temperatures at Nadi Airport has been decreasing, and while a similar trend exists at Suva, it is not statistically significant (Table 4.3).

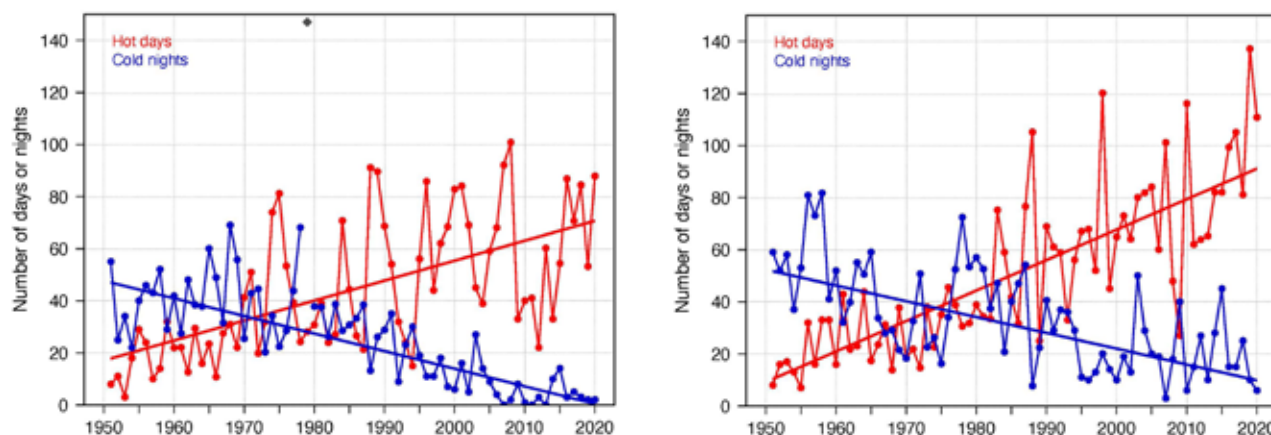
Table 4.3:

Trends in annual temperature extremes at Suva (left) and Nadi Airport (right). The 95% confidence intervals are shown in parentheses, and trends significant at the 95% level are shown in bold. Hot and cool days, and warm and cold nights are measured relative to 1961–1990 (see Chapter 1 for details).

	Suva	Nadi Airport
1951–2020		
Number of hot days (days/decade)	+7.66 (+3.88, +11.64)	+11.69 (+9.72, +13.51)
Number of warm nights (nights/decade)	+14.35 (+10.26, +18.91)	+17.95 (+15.69, +20.17)
Number of cool days (days/decade)	-5.69 (-7.02, 4.27)	-5.62 (-9.53, 1.92)
Number of cold nights (nights/decade)	-6.75 (-8.53, 5.14)	-6.07 (-8.90, 3.26)
Cooling degree days (degree days/decade)	+50.06 (+44.84, +55.32)	+53.98 (+48.70, +60.01)
Daily temperature range (°C/decade)	-0.06 (-0.16, +0.03)	-0.05 (-0.10, 0.01)

Figure 4.7:

Annual number of hot days and cold nights at Suva (left) and Nadi Airport (right). Straight lines indicate linear trends. The magnitudes of the trends are presented in Table 4.3. Diamonds indicate years with insufficient data for one or both variables.



4.6 Tropical cyclones

4.6.1 Seasonal cycle

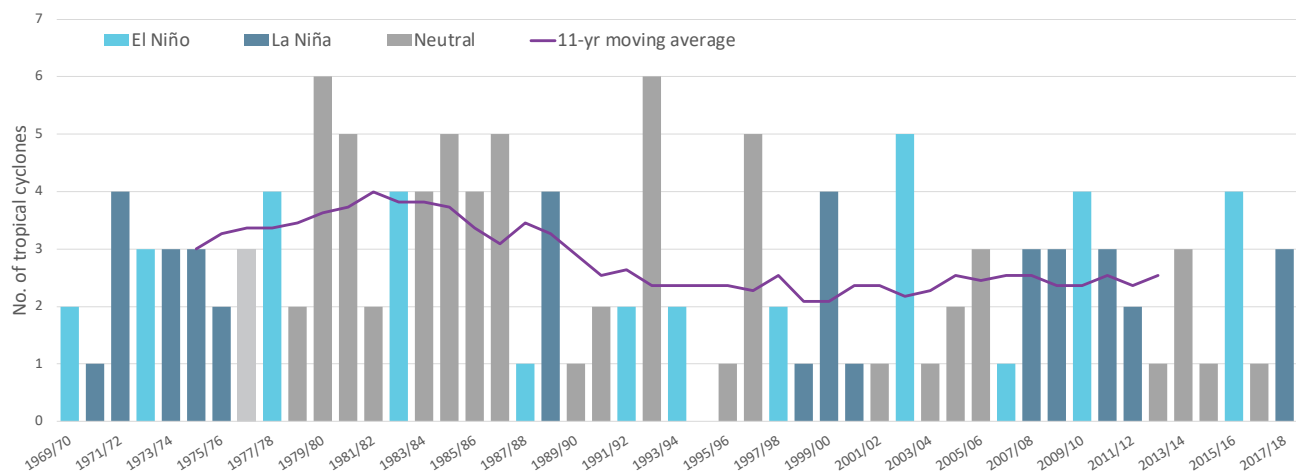
Tropical cyclones usually affect Fiji during the southern hemisphere tropical cyclone season, which is from November to April. Tropical cyclones also occasionally occur in October and May of El Niño years. The tropical cyclone archive of the southern hemisphere indicates that between the 1969/70 and 2017/18 seasons, 135 tropical cyclones (Figure 4.8) passed within the EEZ. This represents an average of 28 cyclones per decade. Tropical cyclones are most frequent in neutral years (29 cyclones per decade), and then equally likely during El Niño and La Niña years (26 cyclones per decade).

Interannual variability in the number of tropical cyclones in the EEZ is large, ranging from zero in the 1994/95 season to six in 1979/80 and 1992/93 (Figure 4.8). High interannual variability and the small number of tropical cyclones occurring in the EEZ make reliable identification of long-term trends in frequency and intensity difficult.

Some tropical cyclone tracks analysed in this section include the tropical depression stage (sustained winds ≤ 34 knots) before and/or after tropical cyclone formation.

Figure 4.8:

Number of tropical cyclones passing within the Fiji EEZ per season. Each season is defined by ENSO status, with light blue being an El Niño year, dark blue a La Niña year and grey showing a neutral ENSO year. The 11-year moving average is presented as a purple line and considers all years.



4.6.2 Trends

Trends in total number of tropical cyclones (<995 hPa) and severe tropical cyclones (<970 hPa) are presented for the period 1981/82–2020/21 for the greater Southwest Pacific (135°E–120°W; 0–50°S). Trends are presented at a regional scale as the number of tropical cyclones occurring within Pacific Island EEZs is insufficient for reliable long-term trend analysis.

For the total number of tropical cyclones, the trend (and 95% confidence interval) is -0.92 ($-1.85, 0.01$) tropical cyclones/decade. There has been little change/marginal decline in the total number of tropical cyclones over the last 40 seasons. This trend is not statistically significant.

For the total number of severe tropical cyclones, the trend is -0.80 ($-1.32, -0.29$) tropical cyclones/decade. There is a negative

trend in the number of severe tropical cyclones over the last 40 seasons. There has been little change/marginal decline in the proportion of tropical cyclones reaching severe status. The trend is -0.04 ($-0.08, 0.00$) tropical cyclones/decade. The negative trend is statistically significant.

Records of tropical cyclones exist from the late 1800s in some countries in the Southwest Pacific, but trends in tropical cyclones have only been presented from 1981/82. Satellite-based observations began in the Southwest Pacific in the early 1970s, but consistent coverage and reliable intensity estimates have only been available since the early 1980s. Confidence in tropical cyclone trends is moderate as the definition of a tropical cyclone has changed and satellite observation methods have continued to improve over the last 40 years.

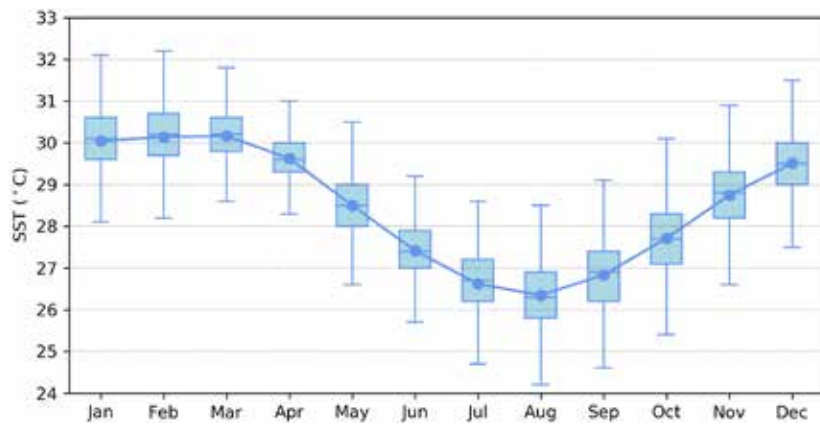
4.7 Sea surface temperature

4.7.1 Seasonal cycle

Ocean temperature, as measured by the Lautoka tide-gauge from 1992 to 2021, reaches on average a maximum of approximately 30 °C from December to March (Figure 4.9),

but individual months can get as high as 32 °C. Minimum average temperature reaches a low of 26.4 °C in August. Temperatures can be up to 2 °C higher or lower than these averages, although 50% of observations fall within 1 °C of the average.

Figure 4.9: Annual temperatures measured at the Lautoka tide-gauge. Blue dots show the monthly average, and shaded boxes show the middle 50% of observations. Lines show the top and bottom 25% of observations.

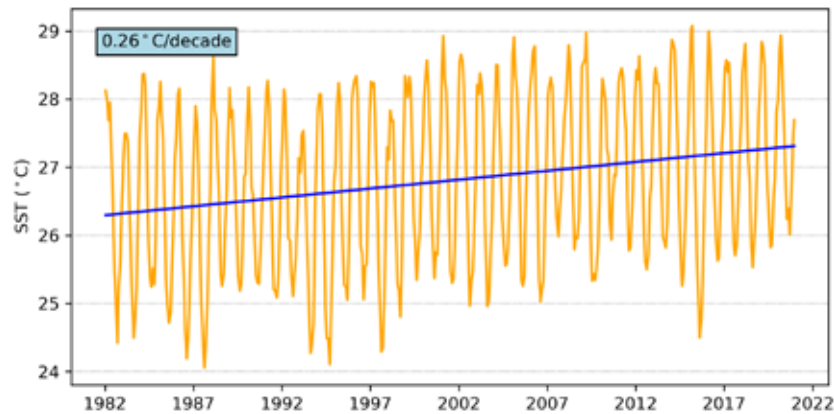


4.7.2 Trends

Historical changes in SST around Fiji are consistent with the broad-scale changes in the region. Water temperatures remained relatively constant from the 1950s to the

late 1980s. This was followed by a period of more rapid warming. Figure 4.10 shows the 1981–2021 SST from satellite observations averaged over the EEZ. The data show a trend of 0.26 °C per decade with a 95% confidence interval of ± 0.10 °C.

Figure 4.10: Sea surface temperature from satellite observations averaged across the Fiji EEZ, shown as the orange line. The blue line shows the linear regression trend.



4.8 Sea level

4.8.1 Seasonal cycle

Fiji experiences a semidiurnal tidal cycle, meaning two high and two low tides per day. The highest predicted tides of the year typically occur during the wet season months of December–February. Figure 4.11 shows the number of hours the 99th percentile (2.39 m) sea level threshold is exceeded per month across the entire sea level record at Lautoka. Peak sea levels

typically occur over a significant portion of the year from October to March. La Niña years typically have higher sea levels outside the austral summer, specifically March/April and September/October.

Since approximately 2009, the number of hours where sea level exceeds the 2.39 m sea level threshold has increased steadily. This is due to a combination of sea-level rise and subsidence occurring at Fiji (Brown et al. 2020).

Figure 4.11: Number of hours exceeding 99th percentile sea level threshold per month from 1992 to 2021 at the Lautoka tide-gauge. Blue shading indicates the number of hours, and the final row provides a percentage summary of all the years.

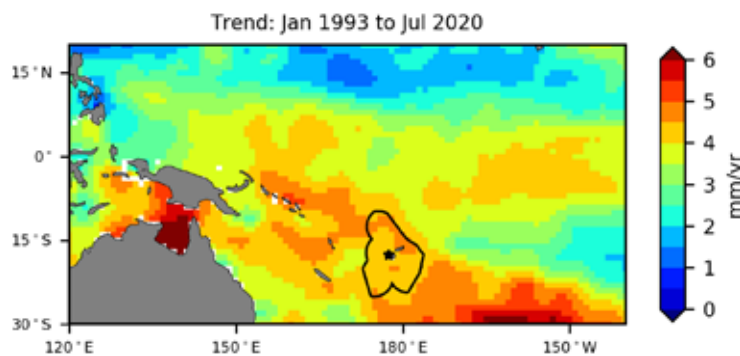
Number of hours exceeding 2.39 m (Lautoka, Fiji)													
	Jan	Feb	Mar	Apr	May	Jun	Jul	Aug	Sep	Oct	Nov	Dec	Annual
1992	0	0	0	0	0	0	0	0	0	0	0	2	2
1993	0	0	0	0	0	0	0	0	0	0	0	0	0
1994	0	0	0	0	0	0	0	0	0	0	0	0	0
1995	0	0	0	0	0	0	0	0	0	0	0	2	2
1996	1	0	0	0	0	0	0	0	0	0	0	0	1
1997	0	4	15	0	0	0	0	0	0	0	0	0	19
1998	0	0	0	0	0	0	0	0	0	0	0	0	0
1999	0	0	0	0	0	0	0	0	0	0	0	0	0
2000	5	0	0	0	0	0	0	0	0	0	0	0	5
2001	0	2	0	0	0	0	0	0	0	0	0	0	2
2002	0	0	0	0	0	0	0	0	0	1	1	0	2
2003	0	0	0	0	0	0	0	0	0	0	0	0	0
2004	0	0	0	0	0	0	0	0	0	0	0	0	0
2005	0	0	0	0	0	0	0	0	0	0	0	0	0
2006	0	0	0	0	0	0	0	0	0	0	0	0	0
2007	0	0	0	0	0	0	0	0	1	0	0	0	1
2008	0	0	0	0	0	0	0	0	0	0	0	1	1
2009	5	3	0	0	0	0	0	1	0	0	0	0	9
2010	2	1	1	0	0	0	0	0	0	0	0	0	4
2011	0	0	1	0	0	0	0	0	5	6	0	0	12
2012	0	0	1	4	6	0	1	0	0	1	2	9	24
2013	7	0	0	0	0	0	0	0	0	0	0	2	9
2014	11	1	0	0	0	0	0	0	0	0	0	0	12
2015	0	3	0	0	0	0	0	0	0	0	6	0	9
2016	0	0	0	0	0	0	0	0	0	1	0	0	1
2017	0	0	0	0	0	0	0	0	0	0	0	0	0
2018	2	2	0	1	0	0	0	0	0	0	0	0	5
2019	0	0	0	0	0	0	0	0	0	2	0	2	4
2020	0	0	0	5	0	0	0	0	0	5	3	2	15
2021	0	0	2	4	1	0	0	0	0	0	2	8	17
Monthly Totals (%)	21	10	13	9	4	0	1	1	4	10	9	18	

4.8.2 Trends

Sea level at Fiji, measured by satellite altimeters (Figure 4.12) since 1993, has risen between 4 and 5 mm per year across the EEZ, with a 95% confidence interval of ± 0.4 mm in the south and up to ± 1.0 mm in the far north. This is larger than the global average of 3.1 ± 0.4 mm per year (von Schuckmann et al. 2021). This rise is partly linked to a pattern related to climate variability from year to year and decade to decade.

Trend estimates at the Lautoka tide-gauge over a similar time span to the altimetry observations (October 1992 to July 2020) are provided in the PSLGM Monthly Data Report for July 2020 (<http://www.bom.gov.au/ntc/IDO60101/IDO60101.202007.pdf>). For Lautoka, the trend is reported as 3.5 mm per year, very similar to the altimetry trends shown in Figure 4.12 (tide-gauge indicated by star symbol).

Figure 4.12: Satellite altimetry annual trend for the Pacific from 1993 to 2020, with the Fiji EEZ highlighted. The star symbol indicates the location of the tide-gauge at Lautoka.



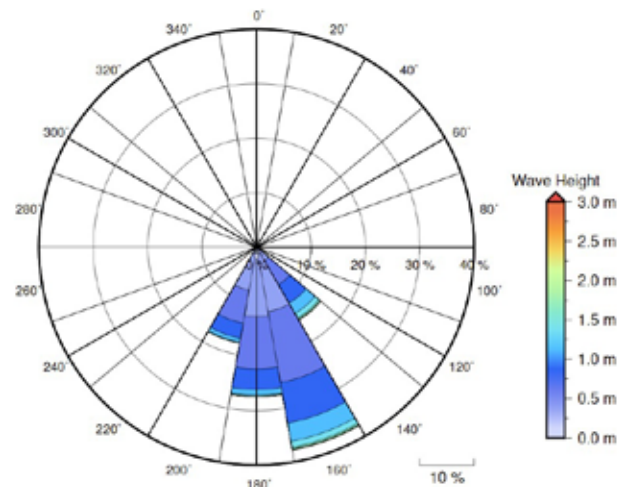
4.9 Waves

4.9.1 Seasonal cycle

The average wave climate at Suva is defined by the significant wave height, peak period and peak direction. The significant wave height is the mean wave height (from trough to crest) of the highest one third of waves and corresponds to the wave height that would be reported by an experienced observer. Peak period is the time interval between two waves of the dominant wave period. Peak direction is the direction from which the dominant waves are coming.

The average sea state is dominated by swells from the south. The annual mean wave height is 0.88 m, the annual mean wave direction is 185° and the annual mean wave period is 12.67 s. In the Pacific, waves often come from multiple directions and for different periods of time. In Suva, there are often more than four different wave direction/period components coming from the southeast to southwest (Figure 4.13).

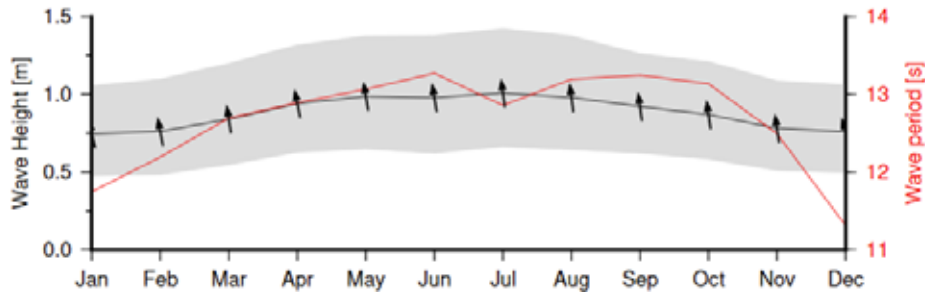
Figure 4.13: Annual wave rose for Suva. Note that direction is where the wave is coming from.



Seasonal wave activity peaks in the winter (June–August) months in terms of both wave height and period (Figure 4.14). This is related to the intensification of the Southern Ocean storm track during the austral winter. Conversely, there is slightly

reduced significant wave height during summer (December–February) months, with wave period reduced significantly during this period.

Figure 4.14: Monthly wave height (black line), wave period (red line) and wave direction (arrows). The grey area represents the range of wave height between calm periods (10% of lowest wave height) and large wave events (10% of highest wave height).

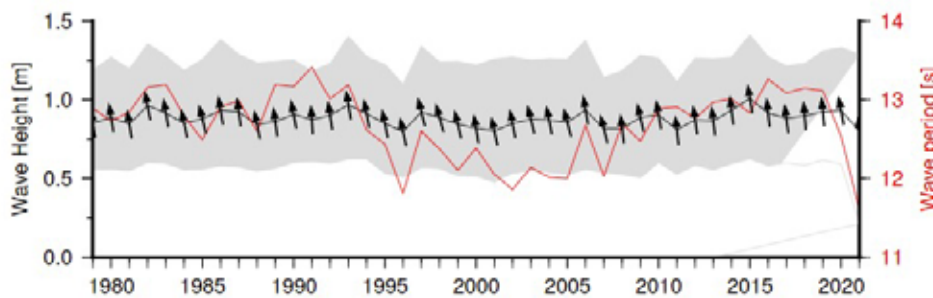


4.9.2 Trends

Waves change from month to month with the seasons, but they also change from year to year with climate oscillations. Typically, these changes are smaller than the

seasonal changes but can be important during phenomena such as ENSO. In Suva, the mean annual wave height has remained unchanged since 1979 (Figure 4.15). The mean annual wave height in Suva is not significantly correlated with the main climate indicators of the region.

Figure 4.15: Annual wave height (black line), wave period (red line) and wave direction (arrows). The grey area represents the range of wave height between calm periods (10% of lowest wave height) and large wave events (10% of highest wave height).



4.9.3 Extreme waves

Extreme wave analysis for Suva was done by defining a severe height threshold and fitting a generalized Pareto distribution (GPD). The optimum threshold selected was 1.97 m. In the 42-year wave hindcast, 112 wave events reached or exceeded this threshold, averaging 2.7 per year. The GPD was fitted to the largest wave height reached during each of these events

(Figure 4.16, Table 4.3). Extreme wave analysis is a very useful tool but is not always accurate because the analysis is very sensitive to the data available, the type of distribution fitted and the threshold used. For example, this analysis does not accurately account for tropical cyclone waves. More in-depth analysis is required to obtain results appropriate for designing coastal infrastructure and coastal hazard planning.

Figure 4.16: Extreme wave distribution for Suva. The crosses represent the wave events that have occurred since 1979. The solid line is the statistical distribution that best fits past wave events. The dashed lines show the upper and lower confidence limits of the fit. There is a 95% chance that the fitted distribution lies between the two dashed lines. Note that the annual return interval is in logarithmic scale.

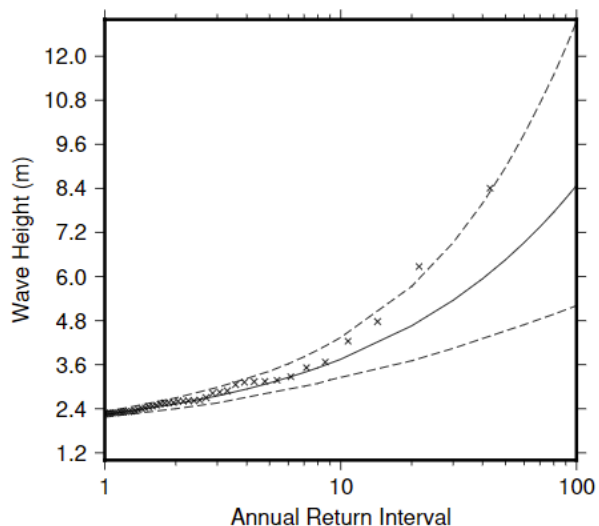


Table 4.3: Summary of the results from extreme wave analysis in Suva

Large wave height (90 th percentile)	1.26 m
Severe wave height (99 th percentile)	1.74 m
1-year ARI wave height	2.24 m
10-year ARI wave height	3.75 m
20-year ARI wave height	4.66 m
50-year ARI wave height	6.46 m
100-year ARI wave height	8.48 m